

Calorimetric Studies of Small-Molecule Adsorption to Carbon Nanotubes

by

Kristin Lena Glab

B.S. Chemistry
Vanderbilt University, 2007

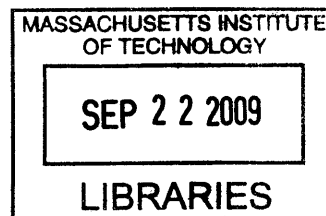
SUBMITTED TO THE DEPARTMENT OF CHEMISTRY IN PARTIAL
FULFILLMENT OF THE REQUIREMENTS FOR THE DEGREE OF

MASTER OF SCIENCE IN CHEMISTRY
AT THE
MASSACHUSETTS INSTITUTE OF TECHNOLOGY

(September)
AUGUST 2009

© 2009 Kristin Lena Glab. All right reserved.

The author hereby grants to MIT permission to reproduce
and to distribute publicly paper and electronic
copies of this thesis document in whole or in part
in any medium now known or hereafter created.



ARCHIVES

Signature of Author: _____
Department of Chemistry
August 28, 2009

Certified by: _____
Timothy M. Swager
Professor of Chemistry
Thesis Supervisor

Accepted by: _____
Robert Warren Field
Robert T. Haslam and Bradley Dewey Professor of Chemistry
Director of Graduate Studies

Calorimetric Studies of Small-Molecule Adsorption to Carbon Nanotubes

by

Kristin Lena Glab

Submitted to the Department of Chemistry
on August 28, 2009 in Partial Fulfillment of the
Requirements for the Degree of Master of Science in
Chemistry

ABSTRACT

Isothermal titration calorimetry (ITC) was developed as a technique for qualitatively comparing the heat of absorption of small molecules to single-walled carbon nanotubes (SWCNTs). In agreement with other studies, it was shown that polyaromatic hydrocarbons (PAHs) that can achieve a greater degree of π -orbital overlap with the curved surface of carbon nanotubes (CNTs) adsorb more strongly. ITC studies also indicated that adsorption of a π -basic metalloaromatic gold pyrazolate trimer, $[\text{Au}(3,5\text{-Et}_2\text{Pz})]_3$, to SWCNTs in DMF is accompanied by a large negative enthalpy change, while the structurally-related π -acidic macrocycle, $[\text{Hg}(\text{C}_6\text{F}_4)]_3$, does not have a large enthalpy of adsorption. This result agrees with previous studies indicating that CNT binding energy depends upon the polarizability of the ligand. Molecules with large CNT binding affinity have potential for use in CNT-based sensing applications, serving to anchor analyte receptors to the surface of CNTs.

In this context, a phosphoresorcin[4]arene decorated with four pendant pyrene moieties was investigated as a bifunctional SWCNT adsorbent and receptor for sensing biogenic amines. Though the cooperative binding effect of the pendant pyrene moieties effectively tethers the cavitand receptor to CNTs, primary ammonium salts do not bind to the cavitand more strongly than to the SWCNT surface. Highly selective receptors with large binding affinities for both CNTs and analyte are necessary to optimize CNT-based sensing technologies. ITC can be useful tool for identifying effective receptor molecules.

Thesis Supervisor: Timothy M. Swager
Title: Professor of Chemistry

ACKNOWLEDGEMENTS

To give anything less than your best is to sacrifice the Gift.

— Steve Prefontaine

First and foremost, Tim's generosity deserves acknowledgement as something incredible. As a principle investigator, he is always ready with new ideas for research projects as new group members arrive and not-so-new group members look to take on different projects. As an inventor, he has shared the fruits of his ideas with all the researchers involved. As a provider, he has supported a large group of researchers for a good number of years and procured many expensive "toys" to facilitate their work. As an advisor, he is ever supportive of his students' short- and long-term goals.

Tim asks for almost nothing in return. The most important factor motivating members of the Swager group is their desire to return Tim's generosity; we want to do our best for Tim because we all know that Tim is doing his best for us. This relationship between Tim and his advisees is what makes the Swager group special.

Next, thanks to the labmates who have made the past year and a half of work at the ISN enjoyable. My hoodmates, Emily Tsui and Yumiko Ito, deserve credit for their ability to keep things neat and organized and keep up with my rambling conversations. Thanks to Armando Ramirez-Monroy for many interesting discussions related to to phonetics, dance, and chemistry. Thanks to Stefanie Sydlik for enthusiastic conversations about music, dance, and rowing. Thanks to Ryan Moslin, the ISN's Jedi knight of synthesis, for deftly dealing with all the questions I threw at him.

I must also thank Elisa Biavardi, whose work initiated the research described in Chapter III; Jeewoo Lim, who helped me with the synthesis of pentacene derivative **1**; and Debby Pheasant, the helpful stewardess of the instruments at the Biophysical

Instrumentation Facility. Thanks to our lab managers, Amy, Caitlin, and Becky, and our administrative assistant, Kathy. Their work keeps the Swager group organized and productive. And thanks to Joe Walish and Daniel Alcazar for carrying on the graphene research started by Wei Zhang, Ryo Shitani, and myself.

Thanks to my former research advisors: Craig Forsyth, who first instilled a love for organic synthesis in me; Piotr Kaszynski, who introduced me to the intricacies of organic materials; and Joe Sly, whose enthusiasm for macromolecular chemistry is infectious. Finally, thanks to the people closest to me, my parents and my husband. Their faith in my potential as a scientist is what keeps me mixing compounds today.

TABLE OF CONTENTS

LIST OF FIGURES	6
INTRODUCTION	8
ADSORPTION TO CARBON NANOTUBES	8
ISOTHERMAL TITRATION CALORIMETRY	9
OBJECTIVES	12
ADSORPTION OF POLYAROMATIC HYDROCARBONS TO SINGLE-WALLED CARBON NANOTUBES	15
TERNARY BINDING STUDIES WITH CAVITANDS, AMINES, AND SINGLE-WALLED CARBON NANOTUBES	21
ADSORPTION OF METALLOAROMATIC COMPOUNDS TO SINGLE-WALLED CARBON NANOTUBES	31
SYNOPSIS	36
EXPERIMENTAL	38
SYNTHESIS	38
ISOTHERMAL TITRATION CALORIMETRY	39
REFERENCES	41

LIST OF FIGURES

Figure 1. Thermodynamic constants ΔH and K_{assoc} , as well as the stoichiometry factor, n , can be measured directly from ITC titration data.

Figure 2. The shape of an ITC titration curve varies with c , that is, the product of the titrand concentration and the titrant/titrand equilibrium constant. Reproduced with permission from W. B. Turnbull.

Figure 3. Optimal geometry of polyaromatic hydrocarbons adsorbed to graphene sheets minimizes electrostatic repulsions by parallel displacement of aromatic rings.

Figure 4. Polyaromatic hydrocarbons used in ITC studies.

Figure 5. ITC plot for the titration of pyrene into SWCNT dispersion with pyrene heat of dilution subtracted (left) and overlay plot of both pyrene heat of dilution and heat of pyrene titration into SWCNT (right).

Figure 6. ITC plot for the titration of tetracene (1.1 mM) into SWCNT dispersion (21.2 mM C atoms) with tetracene heat of dilution subtracted.

Figure 7. ITC plot for the titration of pentacene derivative **1** (0.46 mM) into SWCNT dispersion (21.3 mM C atoms) with the heat of dilution of **1** subtracted.

Figure 8. The phosphonate and thiphosphonate cavitands used in ITC studies.

Figure 9. ITC plots for titration of phosphonate cavitand **2** (0.29 mM (left) and 0.136 mM (right)) into SWCNT dispersions (20.5 mM and 24.5 mM C atoms, respectively).

Figure 10. ITC plot for the titration of histamine into phosphonate cavitand **2** with histamine heat of dilution subtracted (left) and overlay plot of histamine titration into **2** and histamine heat of dilution (right).

Figure 11. ITC plot for the titration of EtNH₃Cl into phosphonate cavitand **2** with EtNH₃Cl heat of dilution subtracted (left) and overlay plot of EtNH₃Cl titration into phosphonate cavitand and EtNH₃Cl heat of dilution (right).

Figure 12. ITC plot for the titration of EtNH₃Cl into thiophosphonate cavitand **3** with EtNH₃Cl heat of dilution subtracted (left) and overlay plot of EtNH₃Cl titration into **3** and EtNH₃Cl heat of dilution (right).

Figure 13. ITC plot for the titration of EtNH₃Cl into SWCNT dispersion with EtNH₃Cl heat of dilution subtracted (left) and overlay plot of EtNH₃Cl titration into SWCNT dispersion and EtNH₃Cl heat of dilution (right).

Figure 14. Organometallic complexes **4** and **5** used in ITC titration experiments.

Figure 15. ITC plot for the titration of mercury complex **4** into SWCNT dispersion with heat of dilution of **4** subtracted (left) and overlay plot of gold complex **4** titration into SWCNT dispersion and heat of dilution of **4** (right).

Figure 16. ITC plot for the titration of gold complex **5** into SWCNT dispersion with heat of dilution of **5** subtracted (left) and overlay plot of gold complex **5** titration into SWCNT dispersion and heat of dilution of **5** (right).

CHAPTER I.

INTRODUCTION

Let us learn to dream, gentlemen, then perhaps we shall find the truth... But let us beware of publishing our dreams till they have been tested by waking understanding.

— (Friedrich) August Kekulé

Adsorption to Carbon Nanotubes

Materials scientists have envisioned many potential applications for carbon nanotubes (CNTs) that take advantage of the material's unique electronic, optical, mechanical, kinetic, and thermal properties. Most of these applications cannot be realized without control and modification of the properties of CNTs. Properties such as length, diameter, chirality, and purity can be controlled to some extent by various methods of synthesis, purification, and separation. Further modification of CNT properties can be achieved by covalent functionalization or by adsorption of polymers or small molecules to the nanotube surface. Non-covalent adsorption has the advantage of preserving the basic graphene structure of the nanotube and thus, many of its favorable electronic properties.

Both liquid- and gas-phase adsorption are possible, but CNT de-bundling and coverage can be better controlled via liquid-phase adsorption.ⁱ Popular small molecules for surface modification of CNTs and fullerenes include polymers, surfactants, biomolecules, and polycyclic aromatic hydrocarbons (PAHs).ⁱⁱ The extent and mechanism of small molecule adsorption to CNTs have been studied by Raman spectroscopy, which demonstrates adsorption of molecules to CNTs through shifts in the radial breathing mode bands, and uv-vis spectroscopy, which can be employed to construct adsorption isotherms.

Adsorption isotherms indicate the equilibrium distribution of adsorbate molecules between liquid phase and solid phase and can be used to determine the thermodynamic constants K_L (Langmuir equilibrium constant), ΔH (enthalpy change), ΔS (entropy change), and ΔG (Gibbs enthalpy of adsorption) associated with the adsorption of small molecules to the surface of CNTs.ⁱⁱⁱ Although these thermodynamic parameters cannot tell us about nonequilibrium systems or the kinetics of adsorption, they are nonetheless invaluable for the quantitative characterization of the energetics of adsorption processes.

The adsorption isotherm, however, is a relatively indirect and imprecise tool for determining thermodynamic parameters as compared to calorimetry, which directly measures heat energy. Moreover, modern calorimeters are highly sensitive and easy to use. They are therefore now routinely used in studies of biochemical thermodynamics and are finding increasing use in other fields of supramolecular chemistry.^{iv}

Isothermal Titration Calorimetry

In an isothermal titration calorimetry experiment, two identical cells are held in a cooling jacket that is 5-10 degrees below the cells' temperature, and power is applied to the cells to maintain them at a defined temperature. The sample cell is filled with a solution of the titrand, and the reference cell is filled with the same solvent as was used to prepare the titrand solution. A pipet with a paddle-shaped tip is filled with the titrant and inserted into the sample cell. During the course of the experiment, the pipet stirs the solution in the sample cell and injects aliquots of titrant at user-defined time intervals. The calorimeter response is recorded as the differential power applied to the sample and reference cells in order to maintain them at the same temperature. When the data is

worked up, the recorded differential power is integrated over each injection time interval, and the molar ratio of titrant to titrand versus ΔH is plotted for each injection event.

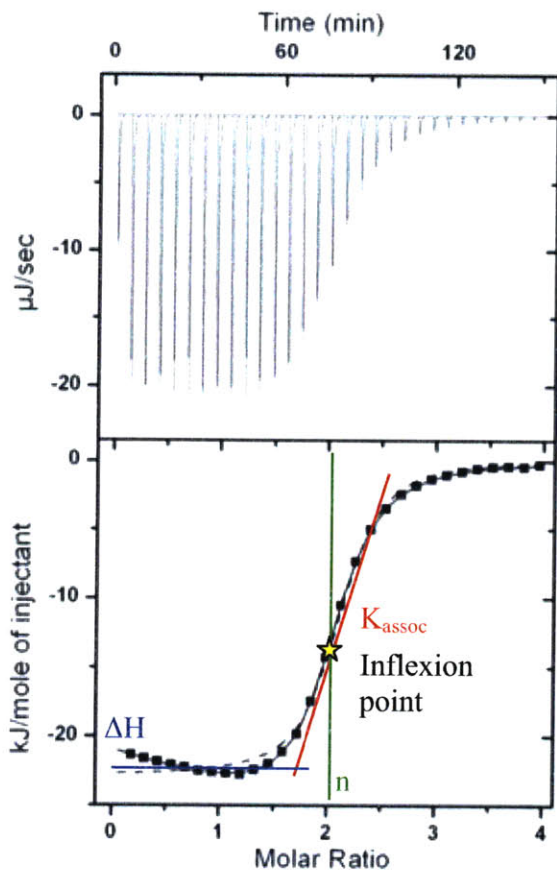


Figure 1. Thermodynamic constants ΔH and K_{assoc} , as well as the stoichiometry factor, n , can be measured directly from ITC titration data.

Ideally, this data can be fit to a sigmoidal-shaped curve from which the enthalpy of binding ΔH , the equilibrium constant K_{assoc} , and the stoichiometric factor n can be extracted (Figure 1). ΔH is simply the extrapolated y-axis intercept, n is the molar ratio at the curve's inflexion point, and K_{assoc} is obtained from the slope of the curve at the inflexion point. Using the thermodynamic relations

$$\Delta G = \Delta H - T\Delta S \text{ and}$$

$$K = e^{-\Delta G/(RT)},$$

the Gibbs enthalpy ΔG and entropy ΔS of binding can be calculated. Additionally, conducting the experiment at multiple temperatures allows one to obtain the heat capacity, ΔC_p .

In order to obtain a sigmoidal-shaped plot for curve fitting, however, the dimensionless value $c = n \times [A]K_{\text{assoc}}$, where $[A]$ is the concentration of titrand in the sample cell, must fall within $5 < c < 500$. Thus, for low binding constants, large titrand concentrations are required, and for large binding constants, low titrand concentrations are required. In the former case, titrand availability and/or solubility can become an issue, while in the latter case, low measured enthalpy values challenge the detection limits of the instrument and result in noisy data. Generally, good data can be obtained for binding constants falling within the range of 10^3 and 10^9 M^{-1} , provided that stoichiometry is well-defined for the process being measured and any competing processes can be deconvoluted.

The problems associated with c -values falling outside the range of $5 < c < 500$ are illustrated in Figure 2. At low c -values, the ITC plot appears flat and relatively featureless, making accurate determination of the inflexion point difficult. At large c -values, the ITC plot appears as a step function, which makes determining the slope of the curve at the inflexion point difficult.

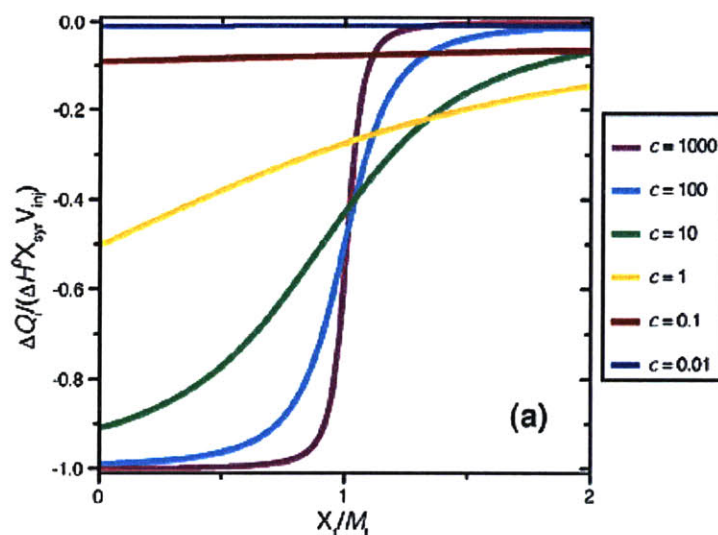


Figure 2. The shape of an ITC titration curve varies with c , that is, the product of the titrand concentration and the titrant/titrand equilibrium constant. Reproduced with permission from W. B. Turnbull.^v

So far, isothermal titration calorimetry has found the most application in the study of biological systems, and thus, aqueous solutions are most commonly used with this technique. Nonetheless, there are multiple examples of ITC studies performed in organic solvents, including methanol, dimethylsulfoxide, acetonitrile, and even less-polar solvents such as chloroform, dichloromethane, tetrachloroethane, toluene.^{vi} Choice of solvent can have a large effect on the thermodynamic binding parameters ΔH and ΔS and therefore should be made carefully. Unfortunately, though, most calorimeters are poorly-equipped to deal with non-polar solvents, as Tygon tubing and O-rings are typically employed in instrument cleaning procedures.

Objectives

There is one reported use of isothermal titration calorimetry to assess adsorption of small molecules to CNTs. In this paper by A. Das *et. al.*, the binding energies of nucleobases with SWCNTs in water were qualitatively compared.^{vii} The ITC plots

obtained by A. Das *et. al* resembled the low-c-value curves shown in Figure 2. They attributed their inability to obtain a sigmoidal shape to the low solubility of CNTs in water.

The objective of this research was to develop isothermal titration calorimetry as a technique for assessing the thermodynamics of small molecule adsorption to single-walled carbon nanotubes. ITC studies were conducted in organic solvent to preclude hydrophobic interactions as the primary driving force for adsorption and to facilitate debundling of CNTs. In particular, dimethylformamide (DMF) was used as the solvent in ITC experiments because of its common usage in CNT experiments, its ability to disperse CNTs, and its moderately high boiling point. The solvent's ability to disperse CNTs is very important for obtaining accurate calorimetric data. When CNTs aggregate, the surface area available for small molecule adsorption and, by extension, the thermodynamic response upon adding adsorbent molecules to the CNT dispersion become limited. Although DMF is moderately effective at dispersing CNTs, N-methylpyrrolidone (NMP) has a larger nanotube dispersion limit and in this respect may have been a better solvent choice.^{viii} At 153 °C, though, the boiling point of DMF is high enough to allow for solution degassing *in vacuo* prior to running ITC experiments without significantly altering the solution concentration. On the other hand, the boiling point of DMF is low enough that solvent removal to recover carbon nanotubes after a titration experiment is not inconvenient. The boiling point of NMP, for comparison, is 202-204 °C. The compatibility of solvents with the ITC's cleaning apparatus, which contains O-rings that quickly degrade in nonpolar solvents, was also considered when choosing solvent in which to run ITC experiments.

Ultimately, it is hoped that non-covalent modification of CNTs with multi-functional molecules will facilitate the development of CNT-based sensing technologies by (a) allowing analyte receptor molecules to be bound to the surface of CNTs and (b) influencing the physical and chemical properties of the CNTs. Polyaromatic hydrocarbons (PAH) are known to adsorb to carbon nanotubes, and ITC studies of PAH adsorption to CNTs are discussed with reference previously-reported non-calorimetric PAH adsorption data in Chapter II. In chapter III, a cavitand decorated with four pyrene moieties is studied as an example of a bifunctional molecule with the ability to both complex ammonium salts and adsorb to the surface of CNTs. The application of such synthetic receptors to CNT-based FET sensors is also discussed. Finally, in chapter IV, the CNT-binding ability of polyaromatic hydrocarbons is compared with the binding abilities of electron-rich and electron-deficient metalloaromatic compounds. Such comparative ITC studies may prove valuable when screening prospective receptor molecules for sufficient CNT- and analyte-binding ability for use in CNT-based sensors.

ADSORPTION OF POLYAROMATIC HYDROCARBONS TO SINGLE-WALLED CARBON NANOTUBES

Could we have entered into the mind of Sir Isaac Newton, and have traced all the steps by which he produced his great works, we might see nothing very extraordinary in the process.

— Joseph Priestley

Studies of liquid-phase adsorption of PAHs to SWCNTs by Gotovac *et. al.* demonstrated that the amount of adsorption depends on the area of overlap between the aromatic π -system of the adsorbing molecule and the nanotube surface.ⁱ For example, tetracene, whose four fused benzene rings can all make contact with the surface of a nanotube when the molecular and nanotube axes are aligned, adsorbs over six times more readily than phenanthrene, whose three fused rings can not all simultaneously overlap with a curved nanotube surface. This observation agrees with theoretical calculations by Grimme^{ix} which indicate that the π - π stacking effect resulting from favorable orbital-dependent dispersion interactions increases nonlinearly with the size of the aromatic π -system. That is, while aromatic systems composed of one or two aromatic rings (i.e., benzene and anthracene) exhibit intermolecular interaction energies comparable to those of their saturated hydrocarbon analogues (i.e., cyclohexane and decalin), aromatic systems of three or more rings exhibit significantly greater intermolecular interaction energies than their hydrocarbon analogues. These favorable interaction energies can be attributed to (a) a minimization of the electrostatic repulsion between π -systems by parallel displacement of the aromatic systems from an eclipsed relationship (Figure 3) and (b) correlations between delocalized π -electrons of two closely stacked polyaromatic systems.

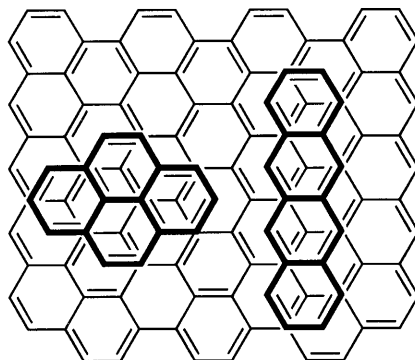


Figure 3. Optimal geometry of polyaromatic hydrocarbons adsorbed to graphene sheets minimizes electrostatic repulsions by parallel displacement of aromatic rings.^x

Though the XPS, Raman, and UV-vis experimental work by Kaneko *et. al.* provided adequate evidence to characterize and quantify PAH adsorption to carbon nanotubes, their studies produced no reliable data on the thermodynamics of PAH adsorption to CNTs. Isothermal calorimetry studies would therefore supplement the techniques used by Kaneko *et. al.* Furthermore, Kaneko *et. al.* only looked at PAH adsorption from toluene dispersions of CNTs; since choice of solvent can have a significant effect on adsorption thermodynamics, comparative studies using amide or chlorinated solvents during adsorption would be enlightening.

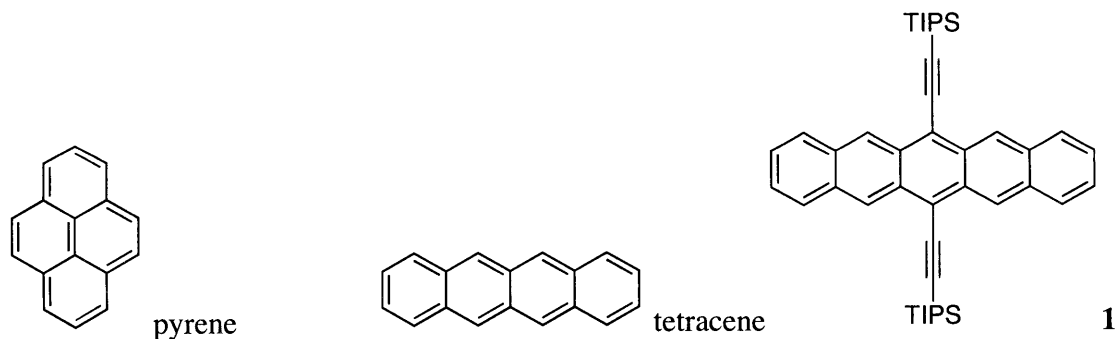


Figure 4. Polyaromatic hydrocarbons used in ITC studies.

Adsorption of pyrene, tetracene, and pentacene derivative **1** (Figure 4) to dispersions of SWCNTs in DMF was studied by isothermal titration calorimetry at 20 °C. Pyrene and tetracene were obtained from commercial sources and used as received.

Pentacene derivative **1** was prepared following a literature procedure.^{xi} ITC plots of heat of adsorption versus molar ratio of adsorbent to SWCNT carbon atoms were generated after subtracting the heat of dilution of the ligand (determined from control experiments) from the heat released upon addition of ligand to suspensions of SWCNTs (Figures 4-6). The CNT suspensions contained concentrations of SWCNT significantly higher than the dispersion limit of CNTs in DMF in order to maximize the available CNT surface area. The ITC data was less noisy and showed greater ligand concentration dependency at high CNT concentrations, though the accuracy of the molar ratios (moles ligand/moles SWCNT C atoms) plotted on the x-axis of the ITC titration plots were likely compromised by CNT bundling. The concentration of each ligand was chosen to optimize the plots of the heat of adsorption versus molar ratio. In the case of tetracene and **1**, however, ligand solubility in DMF (about 0.3 mg/mL for both tetracene and **1**), was the limiting factor.

Remarkably, even at relatively high concentrations of pyrene, only small amounts of heat were released upon addition to SWCNT suspensions (Figure 5). Given that UV-vis, Raman, and microscopy data have all been used to demonstrate that pyrene derivatives adsorb to CNTs, it was surprising to find that in DMF this adsorption process is accompanied by only a small negative enthalpy change. In the case of tetracene (Figure 6), ΔH for each mole of injectant was significantly larger but still not large enough to achieve low noise levels in the plot of ΔH versus molar ratio. For pyrene and tetracene, best fit curves are low and featureless, resembling the $c = 0.01$ and $c = 0.1$ curves in Figure 2. In the case of pyrene, poor data can be primarily attributed to low ΔH for adsorption to CNTs in DMF; little can be said about the binding constant. In the case

of tetracene, both low tetracene solubility and low binding constant must take part of the blame for the noisy data. In the ITC titration curve of pentacene derivative **1** (Figure 7), however, distinct ΔH dependency on ligand concentration can be seen, and the ITC titration plot resembles the $c = 1$ curve in Figure 2.

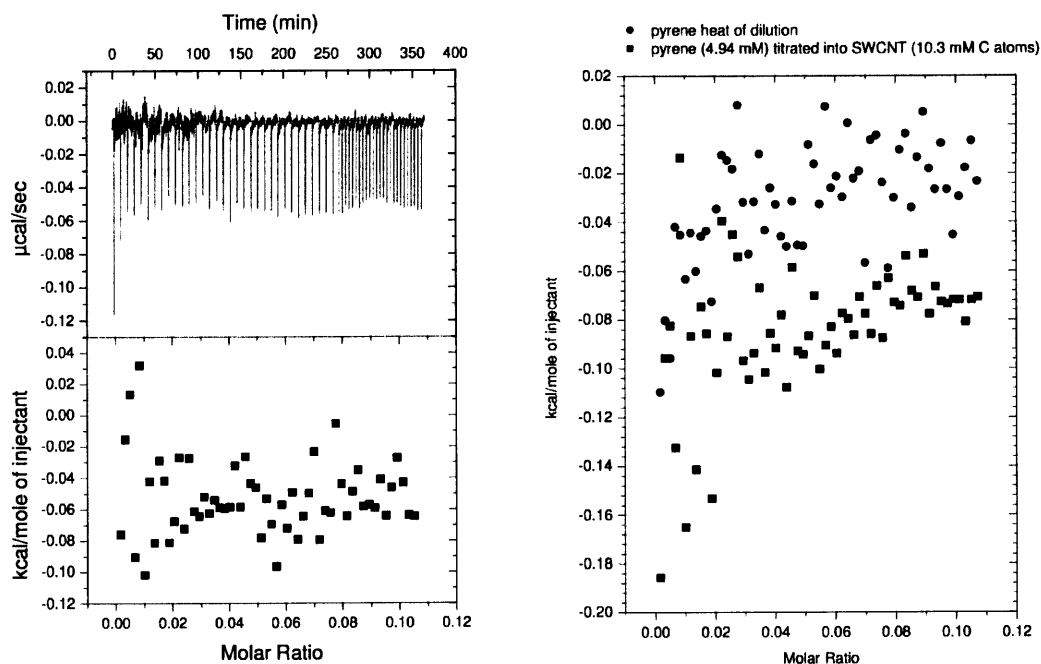


Figure 5. ITC plot for the titration of pyrene into SWCNT dispersion with pyrene heat of dilution subtracted (left) and overlay plot of both pyrene heat of dilution and heat of pyrene titration into SWCNT (right).

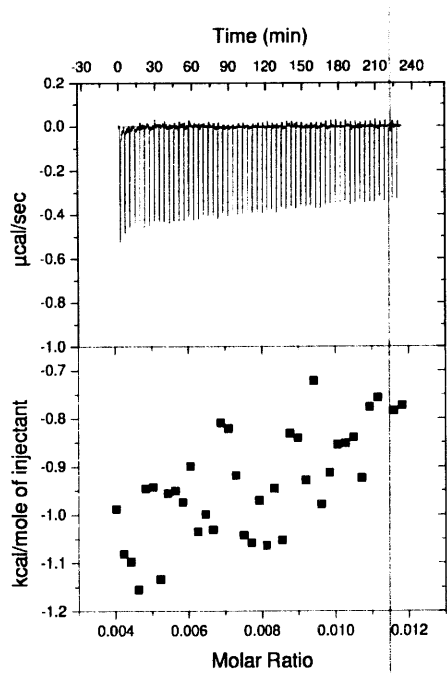


Figure 6. ITC plot for the titration of tetracene (1.1 mM) into SWCNT dispersion (21.2 mM C atoms) with tetracene heat of dilution subtracted.

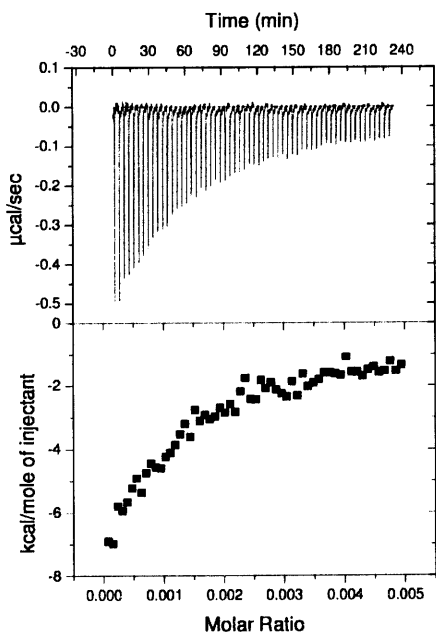


Figure 7. ITC plot for the titration of pentacene derivative **1** (0.46 mM) into SWCNT dispersion (21.3 mM C atoms) with the heat of dilution of **1** subtracted.

By extrapolating best fit curves for the ITC data to zero ligand concentration, the heats of adsorption can be estimated and follow pyrene < tetracene $\ll 1$. Though this sort of analysis is qualitatively enlightening, traditional ligand binding models cannot be used to calculate the enthalpy and entropy of adsorption because the ITC titration curves are not sigmoidal in shape. It is assumed the initial part of the sigmoidal curve is precluded by (a) the limited solubility of CNTs and larger PAHs in DMF, (b) the lack of geometrical or chemical specificity for small molecule binding to the CNT surface, and (c) heterogeneity of CNT surfaces caused by defects, CNT bundling, and differences in diameter and chirality. Limited ligand and substrate solubilities contribute directly to low c -values, and non-specific binding sites can lead to low binding constants as solvent molecules compete with adsorbent molecules for space on the CNT surface. Lack of specificity in the mode of binding also causes ligand/adsorbent stoichiometry to be ill-defined. Defects in the CNT surface may create different binding constants at different sites along the carbon nanotube. Different contact models will also be favored for CNTs of different diameters and chirality. Furthermore, adsorbent molecules will likely interact differently with the outer surface of an isolated CNT as compared to a groove or interstitial site between several bundled CNTs.^{xii} All these characteristics of CNT surfaces should broaden the ITC titration curve, so it is not surprising that a sigmoidal-shaped ITC curve was not observed in these studies.

CHAPTER III.

TERNARY BINDING STUDIES WITH CAVITANDS, AMINES, AND SINGLE-WALLED CARBON NANOTUBES

Few scientists acquainted with the chemistry of biological systems at the molecular level can avoid being inspired. Evolution has produced chemical compounds exquisitely organized to accomplish the most complicated and delicate of tasks. Many organic chemists viewing crystal structures of enzyme systems or nucleic acids and knowing the marvels of specificity of the immune systems must dream of designing and synthesizing simpler organic compounds that imitate working features of these naturally occurring compounds.

— Donald J. Cram

Carbon nanotube-based field-effect transistor (FET) sensors are a promising new class of chemical and biological sensors on account of their high sensitivities, fast response times, and micron-scale device geometries.^{xiii} Naked carbon nanotube arrays have been used in the fabrication of gas sensors, but functionalization of CNTs is necessary to generalize the CNT-based FET device architecture to a broad range of substrates and to increase sensor specificity and sensitivity.^{xiv} There are examples of FET devices employing SWCNTs noncovalently functionalized with DNA, proteins, enzymes, and dextrans which, in turn, act as receptors for particular biological substrates.^{xiii} Of course, few such receptors effectively adsorb to CNTs and selectively complex target substrates. Pyrene moieties are therefore sometimes covalently linked to the biological receptor unit to serve as CNT anchors.^{xv} The constructive π - π stacking interaction between CNTs and pyrene derivatives is well-documented.^{xvi}

Given effective CNT adsorption and substrate binding is achieved, the linker molecule must also cause a shift in the threshold voltage of the FET device upon binding the substrate. This can occur by either changing the linker molecule's ability to transfer charge to the SWCNTs or by changing the linker molecule's ability to alter the SWCNT

charge mobility (i.e. by altering the linker's scattering potential or ability to deform the SWCNTs). Pyrene-based linkers have demonstrated such an ability to alter FET behavior.^{xv}

Though enzymes and many other biological receptor units demonstrate high substrate binding affinity and selectivity, synthetic receptor systems offer chemists more flexibility to choose their substrate and tweak the receptor binding constant. Synthetic receptor systems were first investigated by Pedersen,^{xvii} Lehn,^{xviii} and Cram^{xix} in the form of crown ethers, cryptands, and more complicated macrocycles such as calixarenes, cryptophanes, and cucurbiturils. Calixarenes have emerged as one of the more useful classes of synthetic receptors because of their ability to form inclusion complexes with a wide range of guest compounds.^{xx} By choosing various aldehydes and phenols for the initial cyclooligomerization reaction as well as post-oligomerization functionalization strategies, cavitands of different shape and size, polarity and electrostatic properties can be synthesized. This versatility makes them attractive receptor molecules for chemical sensing.

High levels of histamine in scrombroid fish (i.e. tunas and mackerels) is the most commonly reported cause of seafood poisoning in the United States.^{xxi} Fresh fish do not contain high concentrations of histamine, but in improperly preserved fish, indigenous bacteria containing the enzyme histidine decarboxylase can convert the amino acid histidine into dangerous amounts of histamine.^{xxii} Sensing of biogenic amines is therefore important for the determination of histamine in food. Although chromatographic techniques, fluorometric procedures, immunochemical assays, and direct enzyme-linked immunosorbent assays for detecting histamine are available, none of these tests are

sufficiently cheap, quick, or simple for routine testing. Thus the development of a CNT-based FET sensor for histamine determination could provide a useful immunosensor to the seafood industry.

Phospho(IV)cavitands such as **2** (Figure 8) containing calix[4]resorcinarene macrocycles with phosphonate bridging groups effectively complex hard cations in their bowl-shaped binding cavity.^{xxiii} In particular, the inward-pointing P=O oxygen atoms are known to form a stable acid-base complex with ammonium salts. Thus this class of cavitand may prove to be an effective receptor for sensing biogenic amines such as histamine that exist primarily as ammonium salts at biological pH.^{xxiv} Phospho(IV) cavitand **2** was designed and synthesized by Elisa Biavardi for use in a CNT-based FET ammonium sensor. It was envisioned that the four pendant pyrene units would effectively anchor the cavitand to the CNT surface and that the phosphonate rim of the cavitand would complex ammonium salts. It is important for both of these binding interactions to be greater than that between the ammonium substrate and the CNT surface. If ΔG of the interaction between the cavitand and the CNT surface is less negative than that of the interaction between ammonium salts and the CNT surface, ammonium salts may displace the cavitand from the CNT surface. Additionally, binding of the ammonium salt to free CNT surface rather than to the cavitand binding pocket would convolute the FET response, as it would not be solely a function of ammonium-cavitand complexation.

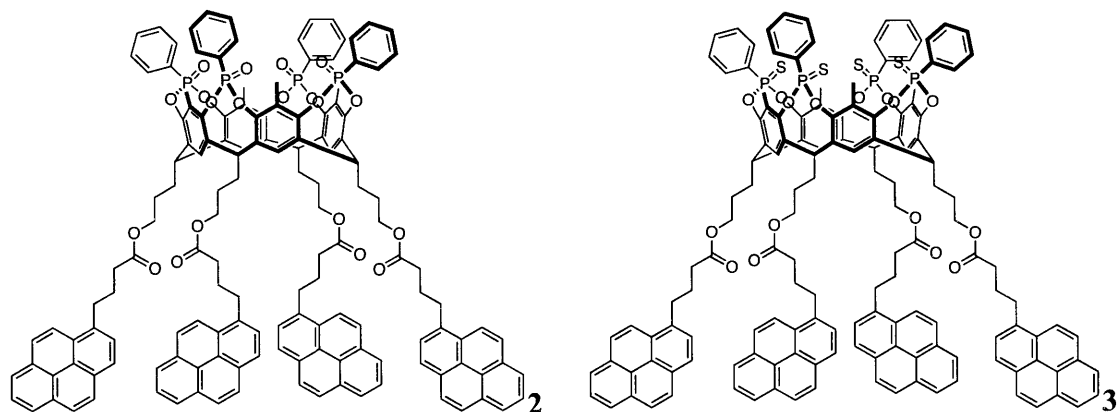


Figure 8. The phosphonate and thiphosphonate cavitands used in ITC studies.

Isothermal titration calorimetry and NMR titration studies were used to study the interactions between phospho(IV)cavitand **2**, SWCNTs, and ammonium salts.

Gratifyingly, it was found that though pyrene itself does not bind to SWCNTs with large ΔH , phosphonate cavitand **2**, decorated with four pyrene moieties, binds to SWCNTs with ΔH of at least -14 kcal/mol **2** (Figure 9). Thus, the cooperative binding of four pyrene units tethered to a macrocycle is much stronger than four independent pyrene molecules isolated in solution. The enthalpy of adsorption of phosphonate cavitand **2** onto SWCNTs is also roughly twice that of pentacene derivative **1**.

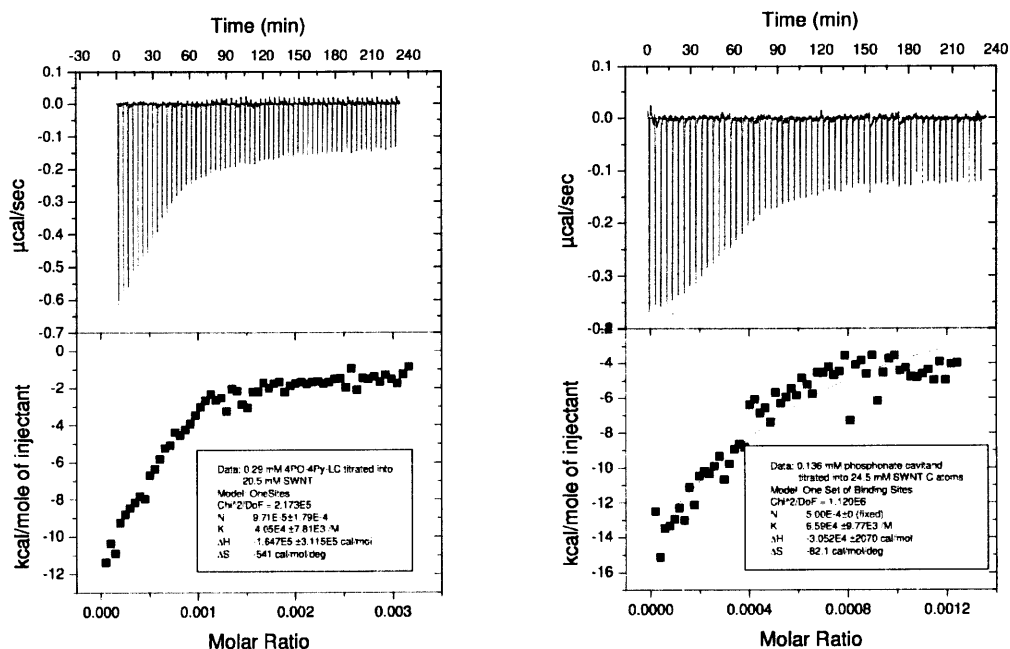


Figure 9. ITC plots for titration of phosphonate cavitand **2** (0.29 mM (left) and 0.136 mM (right)) into SWCNT dispersions (20.5 mM and 24.5 mM C atoms, respectively).

On a [13,9] SWCNT, at most twelve sp^2 carbon atoms and 2.5 aromatic rings of phenanthrene can be in close proximity to the CNT surface at a given time, while all eighteen atoms and four aromatic rings of tetracene can adsorb flush to the CNT surface.¹ By extension, when **2** adsorbs to a moderate-diameter CNT, forty-eight sp^2 carbon atoms and about twelve aromatic rings split over four pyrene moieties can be in close contact with the tube surface at a time. In the case of pentacene derivative **1**, only twenty-two sp^2 carbon atoms and five aromatic rings from the pentacene core can interact with the CNT surface. Considering that adsorption ability increases with the molecular surface area able to interact with the CNT surface, does not seem unreasonable that ΔH for adsorption of cavitand **2** to SWCNTs would be approximately twice that of pentacene **1**.

ITC titration studies with histamine showed that the neutral amine does not complex strongly with phosphonate cavitand **2** in DMF (Figure 10). In the absence of

protic solvent, very little if any histamine is protonated. Phosphonate cavitand **2** complexes with cations, not free amine bases, therefore it is understandable that the ITC curve for titration of histamine into **2** nearly matches the histamine heat of dilution curve.

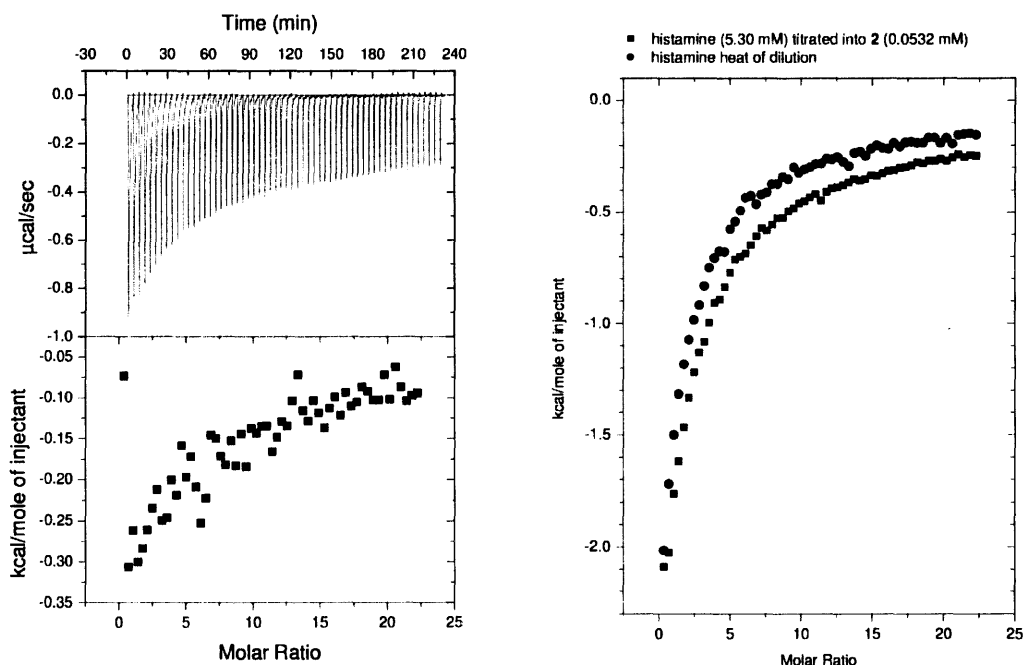


Figure 10. ITC plot for the titration of histamine into phosphonate cavitand **2** with histamine heat of dilution subtracted (left) and overlay plot of histamine titration into **2** and histamine heat of dilution (right).

Ammonium salts of histamine are insoluble in DMF, so ethylammonium chloride was used in ITC studies of ammonium complexation with **2**. As can be seen in Figure 11, the difference between the ITC curve for EtNH₃Cl titration into a solution of **2** and the heat of dilution of EtNH₃Cl is not large, but it is well-defined and reproducible. Thiophosphonate cavitand **3** does not complex ammonium salts,^{xxiii} so it was used in a control experiment. The difference between the ITC response for titration of EtNH₃Cl into thiophosphonate cavitand **3** and the heat of dilution of EtNH₃Cl is smaller, more

noisy, and less reproducible (Figure 12) in comparison to the complexation experiment conducted with phosphonate cavitand **2**.

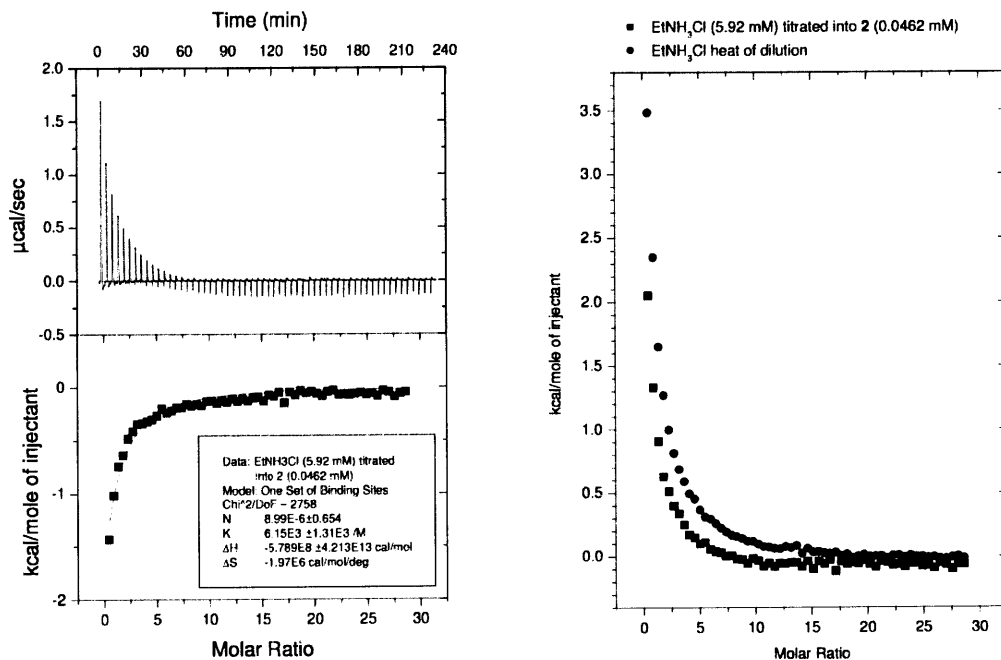


Figure 11. ITC plot for the titration of EtNH₃Cl into phosphonate cavitand **2** with EtNH₃Cl heat of dilution subtracted (left) and overlay plot of EtNH₃Cl titration into phosphonate cavitand and EtNH₃Cl heat of dilution (right).

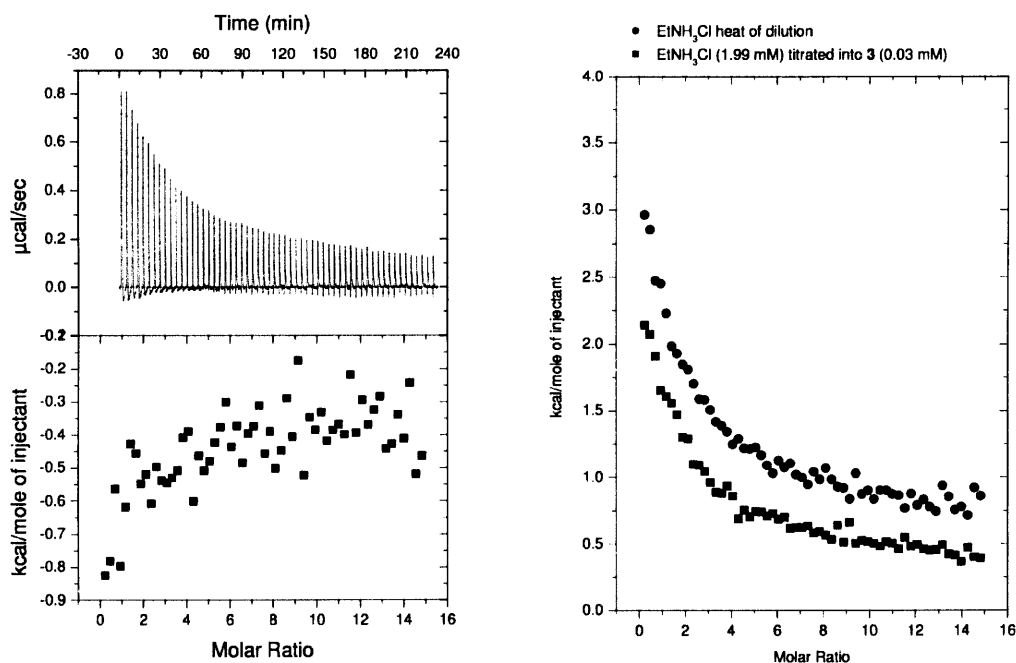


Figure 12. ITC plot for the titration of EtNH₃Cl into thiophosphonate cavitand **3** with EtNH₃Cl heat of dilution subtracted (left) and overlay plot of EtNH₃Cl titration into **3** and EtNH₃Cl heat of dilution (right).

Regrettably, however, titration of EtNH₃Cl into dispersions of SWCNTs indicates that the interaction of ammonium salts with CNTs is stronger than the interaction of EtNH₃Cl with phosphonate cavitand **2** (Figure 13). Amines are known to adsorb to CNT surfaces,^{xxv} and it's likely that at equilibrium, a fraction of ethylammonium species are deprotonated by the Lewis-basic oxygen of DMF, revealing the free amine base for adsorption to SWCNTs. Even at high concentrations of cavitand **2**, it is likely that there will always be free CNT surface available for non-specific amine-CNT adsorption.

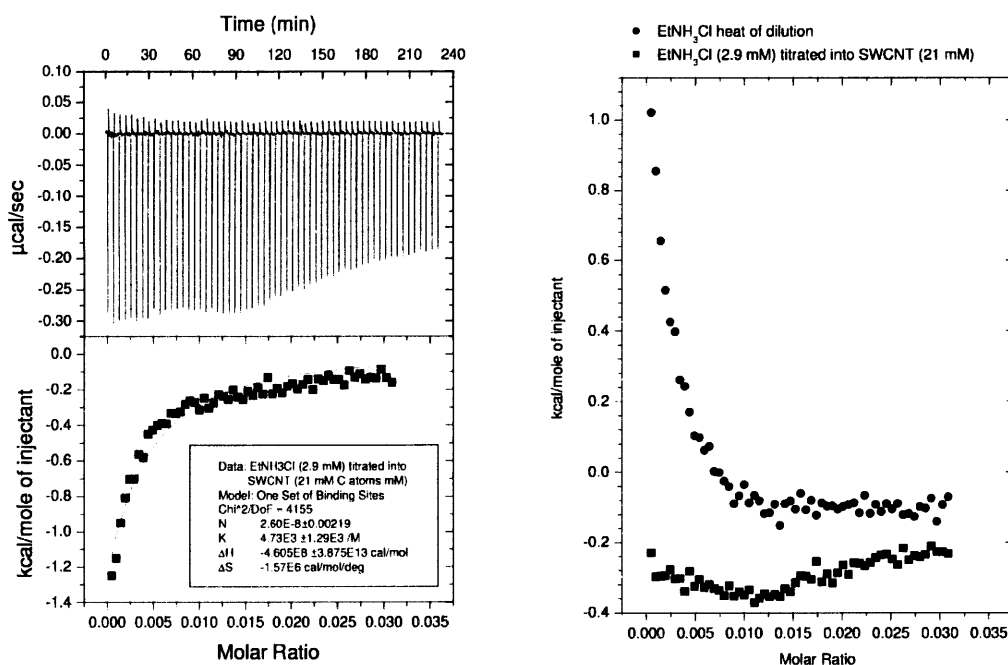


Figure 13. ITC plot for the titration of EtNH₃Cl into SWCNT dispersion with EtNH₃Cl heat of dilution subtracted (left) and overlay plot of EtNH₃Cl titration into SWCNT dispersion and EtNH₃Cl heat of dilution (right).

Consolation may be taken in the fact that cavitand **2** binds to SWCNTs much more strongly than amines, so the amines are unable to displace the cavitand. The thermodynamic data provided by ITC was corroborated by visual evidence. Addition of **2** to SWCNT dispersions caused the CNTs to form aggregates that could not be broken up by sonication. Treating the aggregates with excess EtNH₃Cl and further sonication did not allow the aggregates to be broken up. In contrast, treating a dispersion of SWCNTs with a mixture of solution of both EtNH₃Cl and phosphonate cavitand **2** does not allow aggregates to form. Possibly, the adsorption of **2** to the SWCNT surface is kinetically slower than adsorption of amines. Once amines have partially covered the CNT surface, not enough space may be available for all four pyrene moieties of **2** to adsorb at once, and aggregate formation is precluded.

This study demonstrates that highly selective receptors with large binding affinities for both CNTs and analyte are necessary to optimize CNT-based sensing technologies. ITC can be useful tool for identifying effective receptor molecules.

CHAPTER IV.

ADSORPTION OF METALLOAROMATIC COMPOUNDS TO SINGLE-WALLED CARBON NANOTUBES

...the more accurate the calculations became, the more the concepts tended to vanish into thin air.

— Robert S. Mulliken

Macrometallocyclic trinuclear complexes of the type $[M(\mu-L)]_3$ may be synthesized with a wide range of π -acidity and π -basicity, supramolecular host/guest chemistry, and metal-organic optoelectronic properties by substituting various metals, ligands, and ligand substituents.^{xxvi} By tuning the frontier molecular orbitals of such metalloaromatic compounds, interactions with the π -orbital array of CNTs may be optimized to facilitate adsorption and modify the CNTs' electronic properties. Compounds **4** and **5** were targeted as readily accessible π -acidic and π -basic complexes for ITC studies (Figure 14). Significantly, the inner metalloaromatic rings of the two compounds are isoelectronic – both contain d^{10} metals (Hg(II) and Au(I)), and both contain aromatic bridging ligands. The molecular weights of **4** and **5** are within 10% of each other, at 1045.95 and 960.43 g/mol, respectively, so the inherent potential for van der Waals interactions should be similar for these compounds with CNTs. Mercury complex **4** was prepared as reported in literature^{xxvii} and gold complex **5** was prepared following an analogous procedure^{xxviii}.

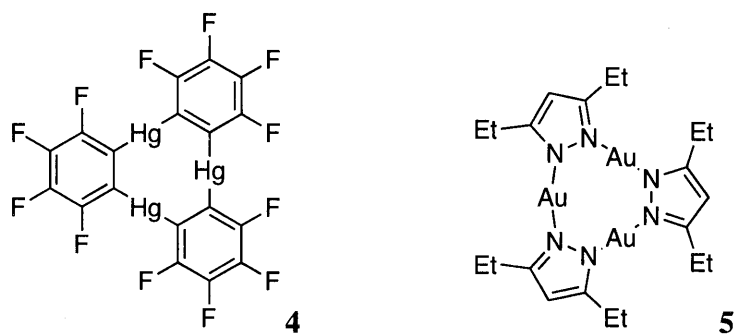


Figure 14. Organometallic complexes **4** and **5** used in ITC titration experiments.

Carbon nanotubes are known to behave as both electron-donors and as electron-acceptors,^{xix} so it is not unreasonable to suspect that both π -acidic compound **4** and π -basic compound **5** could form strong Lewis acid-base interactions with CNTs. However, ITC titration curves (Figures 15 and 16) demonstrate that only π -basic compound **5** has a large negative enthalpy for adsorption to CNTs. The heat released upon titrating mercury complex **4** into SWCNTs is recognizably greater than the heat of dilution of **4**, but only amounts to 1-2 kcal/mol at low ligand concentrations. In contrast, gold complex **5** demonstrates the largest CNT-binding enthalpy of any of the molecules discussed in this thesis – about -30 kcal/mol at low ligand concentrations. That's approximately twice the adsorption enthalpy demonstrated for phosphonate cavitand **2**.

It is also significant that the thermal response upon addition of **5** to SWCNTs is significantly slower than the thermal response of other ligands. Injections were made at 480 second intervals rather than the usual 240 second intervals to allow heat flow to reach baseline levels before each subsequent injection. As ΔH with each injection falls to zero at larger concentrations of **5**, the time required to reach baseline levels of heat flow also decreases. The triangular shape of the peaks in the ITC titration plot may indicate

that adsorption of **5** to SWCNTs is kinetically slow or that a second event – such as aggregation – is happening after adsorption.^{iv}

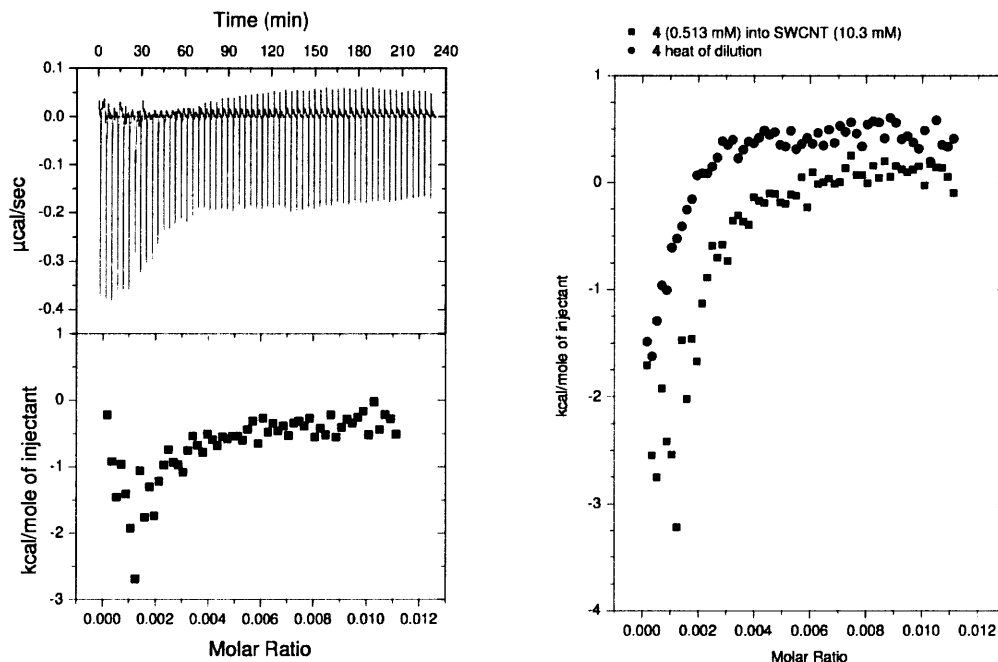


Figure 15. ITC plot for the titration of mercury complex **4** into SWCNT dispersion with heat of dilution of **4** subtracted (left) and overlay plot of gold complex **4** titration into SWCNT dispersion and heat of dilution of **4** (right).

Fitting the ITC titration data of complex **5** using the One Set of Binding Sites model gave a best fit curve with the smallest errors in the values of n , K , and ΔH of any of the SWCNT ligands discussed in this work. With a calculated binding constant of approximately 9×10^4 , the value of K falls well within the range of reasonable binding constants for obtaining quality data from ITC experiments. The value of n , 0.002, indicates a stoichiometry of one adsorbent molecule **5** per 500 SWCNT carbon atoms. It is important to keep in mind that the concentration of SWCNTs used was above the dispersion limit of SWCNTs in DMF. Thus, due to CNT bundling, only a fraction of the total SWCNT surface area was exposed to the solvent and available for ligand binding.

Furthermore, it is known that some adsorbent molecules promote debundling of the CNTs; if this occurred, the surface area available for ligand binding may not have decreased linearly with increasing molar ratio of **5** to SWCNTs.

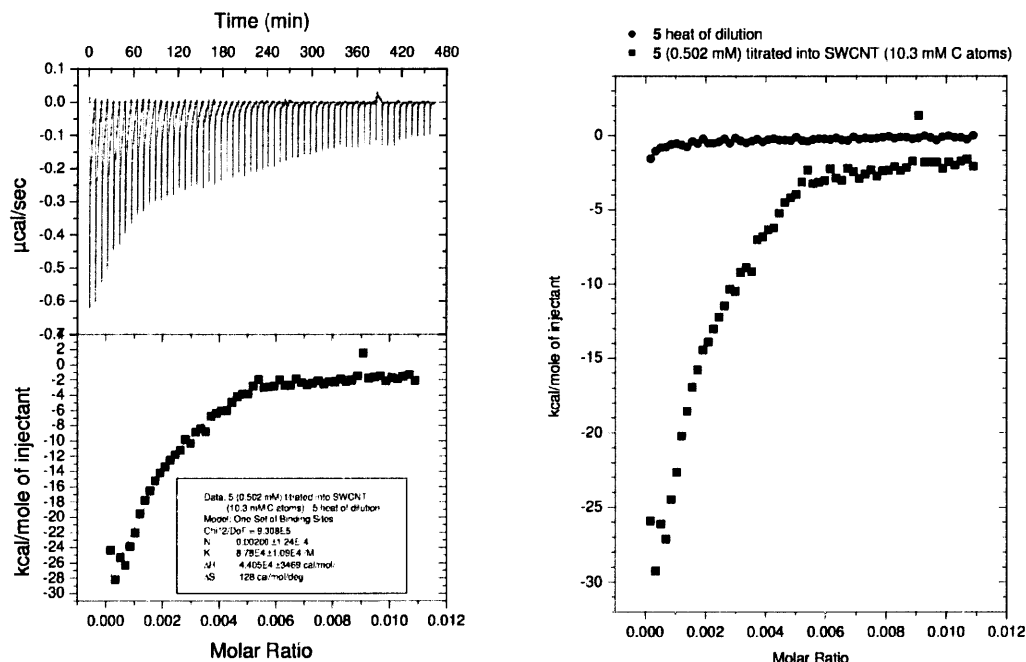


Figure 16. ITC plot for the titration of gold complex **5** into SWCNT dispersion with heat of dilution of **5** subtracted (left) and overlay plot of gold complex **5** titration into SWCNT dispersion and heat of dilution of **5** (right).

An enthalpy change of -44 kcal/mol of **5** adsorbed was calculated by the binding model. The most negative value directly recorded was greater than -30 kcal/mol, so the calculated value may be more negative than the true value but is not unreasonable. Repeating the experiment with less concentrated tirant solution would provide a better sense of the true adsorption enthalpy since the extrapolation to zero ligand concentration would be made from lower molar ratio data points.

The negative calculated entropy value indicates that the total rotational and translational freedom gained by displacement of DMF molecules from the SWCNT

surface is less than the rotational and translational freedom sacrificed by **5** upon binding to the SWCNT surface. This can be rationalized by envisioning that **5** is much more tightly bound to the surface of the CNT than the displaced solvent molecules were.

Now to address the fundamental question brought up by these experimental results: why is the ΔH for binding π -basic metalloaromatic compound **5** to SWCNTs very large, while the ΔH for binding the isoelectronic but π -acidic metalloaromatic compound **4** is remarkably small in comparison to ΔH for PAH **1**, another large aromatic molecule? Theoretical calculations on the adsorption of aromatic compounds to graphene and SWCNTs has demonstrated a direct correlation between the strength of interaction between small aromatic systems with graphene surfaces and the polarizability of the aromatic molecule.^{xxx} Thus, for more extended π -systems and more electron-rich molecules, the strength of small molecule binding to CNTs will be greater. This prediction agrees with the results of ITC titration experiments.

CHAPTER V.

SYNOPSIS

One never notices what has been done; one can only see what remains to be done.

— Marie Curie

Isothermal titration calorimetry was developed as a technique for qualitatively comparing the heat of absorption of small molecules to CNTs. In agreement with other studies, it was shown that PAHs that can achieve a greater degree of π -orbital overlap with the curved surface of CNTs adsorb more strongly. ITC studies also indicated that adsorption of π -basic metalloaromatic compound **5** to SWCNTs in DMF is accompanied by a large negative enthalpy change, while π -acidic macrocycle **4** does not adsorb strongly. This supports previous studies indicating that CNT binding energy depends upon the polarizability of the ligand. To provide a more complete picture of the CNT anchoring abilities of these compounds, XPS, Raman, and UV-vis data should be acquired for SWNTs adsorbed with pentacene derivative **1** and metalloaromatic complexes **4** and **5**. Furthermore, theoretical calculations of the relative polarizabilities and frontier molecular orbital energy levels of **1**, **4**, and **5** would provide more insight into their disparate adsorption abilities.

Future work aims to extend the sensing applications of SWCNTs using rationally-designed analyte receptors. Investigations into the use of metalloaromatic complex **5** in sensing devices may begin with binding studies analogous to those of chapter III and involving **5**, SWNTs, and mercaptans, since gold complexes coordinate strongly with sulfur compounds. However, mercaptans also coordinate strongly with CNT surfaces,^{xxx} so it may be difficult to preclude mercaptan adsorption to CNTs in favor of coordination with gold complex **5**. This problem was confronted when energies of binding of

ammonium salts to **2** and to SWCNTs and were compared in chapter III. Complications associated with non-specific adsorption of analytes to CNT surfaces rather than to the analyte receptors indicate that CNT-based sensing technologies are best suited for sensing analytes which do not have CNT strong binding affinities.

EXPERIMENTAL

The chemists are a strange class of mortals, impelled by an almost insane impulse to seek their pleasures amid smoke and vapour, soot and flame, poisons and poverty; yet among all these evils I seem to live so sweetly that I would rather die than change places with the king of Persia.

— Johann Joachim Becher

Synthesis

Tris(μ -2,3,4,5-tetrafluorophenyl-1,2)trimercury(II) **4**

Trinuclear mercury complex **4** was prepared as described by Sartori et.al.^{xxvii} Mercury(II) acetate (13.4 g, 42 mmol) and glacial acetic acid (1.5 mL) were dissolved in deionized water (200 mL). A solution of tetrafluorophthalic acid (10.0 g, 42 mmol) in deionized water (200 mL) was added to the mercury(II) solution, and a white precipitate formed immediately. The milky mixture was filtered to yield a white, pasty solid. The solid material was added to a sublimation apparatus with a water-cooled cold finger and sublimed at 220 °C (sand bath) and under a dynamic vacuum at 0.05 torr. The unsublimable material was discarded and the sublimed product was returned to the well of the sublimation apparatus. The material was sublimed and re-sublimed at 300 °C, yielding fluffy white crystals (10.3 g, 70 % overall yield). Final purification was performed by recrystallizing the product from hexane, methylene chloride, and a small amount of DMF to produce large, colorless rhombic crystals. FTIR: 1610 m, 1580 m, 1470 sst, 1380 m, 1360 m, 1325 st, 1290 st, 1250 st, 1210 m, 1090 sst, 1050 m, 1005 sst, 940 m, 815 st, 770 m, 640 m, 470 m, 400 m, 370 cm⁻¹ st. ESI-MS: m/z 1045.88 (M). ¹⁹F NMR (300 MHz, acetone-d⁶): δ_F -160, -121.

Tris(μ -3,5-diethylpyrazolato- N,N')trigold(I) **5**

An aqueous solution of potassium hydroxide (30 mg KOH/3 mL H₂O) was added dropwise to a suspension of 3,5-diethylpyrazole (110 mg, 0.89 mmol) and dimethylsulfidegold(I)chloride (226 mg, 0.77 mmol) in methanol (10 mL). A purple-black precipitate formed, and the reaction was stirred for 1 h at room temperature. The solvent was removed *in vacuo*, and the crude product was chromatographed (4:1 hexane/dichloromethane). The product was recrystallized from hexane to yield fine colorless needles (yield). FTIR: 2960, 2920, 2850, 1720, 1530, 1460, 1375, 1250, 1170, 980, 760, 670 cm⁻¹; ESI-MS: m/z 960.2 (M), 1921.3 (2M + 1), 1943.3 (2M + 23); and ¹H NMR (300 MHz, CDCl₃): δ_H 1.3 (t, 18H), 2.7 (q, 12H), 6.2 (s, 3H).

SWCNTs were obtained from Unidyne Carbon Nanotubes Grade/Lot #P0900 and cleaned by (a) refluxing in nitric acid (2.5 M), filtering, washing with water until pH 5, and drying 1 h at 300 °C or (b) sonicating in concentrated HCl, filtering, washing with water until pH 6, and drying *in vacuo* for one day. SWCNTs cleaned by procedure (a) were used in the experiments of chapter III; procedure (b) was used to clean SWCNTs used in the experiments of chapters II and IV.

Isothermal Titration Calorimetry

Isothermal titration calorimetry experiments were conducted using a VP-ITC MicroCal titration calorimeter. In a typical experiment, SWCNTs were dispersed in dry DMF (approx. 0.1 – 0.2 mg/mL) by sonicating for 1 h, and a solution of titrant was prepared using DMF from the same source (approx. 0.5 – 5 mM). The calorimeter was

rinsed with DMF (250 mL) prior to use, and the titrant solution (0.6 mL), titrand solution (2.0 mL), and DMF (2.0 mL) were degassed *in vacuo* for 10 minutes. The degassed DMF was loaded into the reference cell, the titrand solution loaded into the sample cell, and the titrant solution drawn into the calorimeter's pipet. After the cells equilibrated at 20 °C, the pipet stirred at 310 rpm and the titrant solution was added to the sample cell in 5- μ L aliquots every 240 seconds fifty-eight times. In titration experiments using gold complex **5**, 480-second time intervals were required to allow equilibration before each successive injection. The experiment was repeated using neat DMF in the sample cell so that the heat of dilution of the titrant could be subtracted from the host titration thermogram. Data fitting (where appropriate) was performed using ORIGIN (Version 7.0, MicroCal, LLC ITC) and the One Set of Binding Sites model..

REFERENCES

- ⁱ (a) Gotovac, S.; Honda, H.; Hattori, Y.; Takahashi, K.; Kanoh, H.; Kaneko, K. Effect of Nanoscale Curvature of Single-Walled Carbon Nanotubes on Adsorption of Polycyclic Aromatic Hydrocarbons. *Nano Lett.* **2007**, *7*, 583-587. (b) Gotovac, S.; Yang, C.-M.; Hattori, Y.; Takahashi, K.; Kanoh, H.; Kaneko, K. Adsorption of Polyaromatic Hydrocarbons on Single Wall Carbon Nanotubes of Different Functionalities and Diameters. *J. Colloid Interface Sci.* **2007**, *314*, 18-24.
- ⁱⁱ Tasis, D.; Tagmatarchis, N.; Bianco, A.; Prato, M. Chemistry of Carbon Nanotubes. *Chem. Rev.* **2006**, *106*, 1105-1136.
- ⁱⁱⁱ Kuo, C.-Y.; Wu, C.-H.; Wu, J.-Y. Adsorption of Direct Dyes from Aqueous Solutions by Carbon Nanotubes: Determination of Equilibrium, Kinetics, and Thermodynamics Parameters. *J. Colloid Interface Sci.* **2008**, *327*, 308-315.
- ^{iv} Schmidtchen, F. P. Isothermal Titration Calorimetry in Supramolecular Chemistry. *Analytical Methods in Supramolecular Chemistry*. Ed. Schalley, C. Wiley-VCH Verlag GmbH & Co. KGaA: Weinheim, **2007**. 55-78.
- ^v Turnbull, W. B.; Daranas, A. H. On the Value of c : Can Low Affinity Systems be Studied by Isothermal Titration Calorimetry? *J. Am. Chem. Soc.* **2003**, *125*, 14859-14866.
- ^{vi} For example: (a) Chekmeneva, E.; Hunter, C. A.; Packer, M. J.; Turega, S. M. Evidence for Partially Bound States in Cooperative Molecular Recognition Interfaces. *J. Am. Chem. Soc.* **2008**, *130*, 17718-17725. (b) Rossi, S.; Kyne, G. M.; Turner, D. L.; Wells, N. J.; Kilburn, J. D. A Highly Enantioselective Receptor for *N*-Protected Glutamate and Anomalous Solvent-Dependent Binding Properties. *Angew. Chem. Int. Ed.* **2002**, *41*, 4233-4236. (c) Linton, B. R.; Goodman, S. M.; Fan, E.; van Arman, S. A.; Hamilton, A. D. Thermodynamic Aspects of Dicarboxylate Recognition by Simple Artificial Receptors. *J. Org. Chem.* **2001**, *66*, 7313-7319.
- ^{vii} Das, A.; Sood, A.K.; Maiti, P.; Das, M.; Varadarajan, R.; Rao, C.N.R. Binding of nucleobases with single-walled carbon nanotubes: Theory and experiment. *Chem. Phys. Lett.* **2008**, *453*, 266-273.
- ^{viii} Kim, D. S.; Nepal, D.; Geckeler, K. E. Individualization of Single-Walled Carbon Nanotubes: Is the Solvent Important? *Small* **2005**, *1*, 1117-1124.
- ^{ix} Grimme, S. Do Special Noncovalent π - π Stacking Interactions Really Exist? *Angew. Chem. Int. Ed.* **2008**, *47*, 3430-3434.
- ^x Florio, G. M.; Werblowsky, T. L.; Müller, T.; Berne, B. J.; Flynn, G. W. Self-Assembly of Small Polycyclic Aromatic Hydrocarbons on Graphite: A Combined Scanning Tunneling Microscopy and Theoretical Approach. *J. Phys. Chem. B* **2005**, *109*, 4520-4532.
- ^{xi} Anthony, J. E.; Eaton, D. L.; Parkin, S. R. A Road Map to Stable, Soluble, Easily Crystallized Pentacene Derivatives. *Org. Lett.* **2002**, *4*, 15-18.
- ^{xii} Kondratyuk, P.; Yates, J. T. Molecular Views of Physical Adsorption Inside and Outside of Single-Wall Carbon Nanotubes. *Acc. Chem. Res.* **2007**, *40*, 995-1004.
- ^{xiii} Zhao, Y.-L.; Hu, L.; Stoddart, J. F.; Grüner, G. Pyrenecyclodextrin-Decorated Single-Walled Carbon Nanotube Field-Effect Transistors as Chemical Sensors. *Adv. Mater.* **2008**, *20*, 1910-1915.

-
- ^{xiv} Zhang, T.; Mubeen, S.; Myung, N. V.; Deshusses, M. A. Recent Progress in Carbon Nanotube-Based Gas Sensors. *Nanotechnology* **2008**, *19*, 332001.
- ^{xv} (a) Besteman, K.; Lee, J.-O.; Wiertz, F. G. M.; Heering, H. A.; Dekker, C. *Nano. Lett.* **2003**, *3*, 727-730. (b) Li, C.; Curreli, M.; Lin, H.; Lei, B.; Ishikawa, F. N.; Datar, R.; Cote, R. J.; Thompson, M. E.; Zhou, C. *J. Am. Chem. Soc.* **2005**, *127*, 12484-12485. (c) Ogoshi, T.; Takashima, Y.; Yamagushi, H.; Harada, A. *J. Am. Chem. Soc.* **2007**, *129*, 4878-4879. (d) Zhao, Y.-L.; Hu, L.; Stoddart, J. F.; Grüner, G. Pyrenecyclodextrin-Decorated Single-Walled Carbon Nanotube Field-Effect Transistors as Chemical Sensors. *Adv. Mater.* **2008**, *20*, 1910-1915.
- ^{xvi} (a) Tournus, F.; Latil, S.; Heggie, M. I.; Charlier, J.-C. π -Stacking Interaction Between Carbon Nanotubes and Organic Molecules. *Phys. Rev. B* **2005**, *72*, 075431. (b) Britz, D. A.; Khlobystov, A. N. Noncovalent Interactions of Molecules with Single Walled Carbon Nanotubes. *Chem. Soc. Rev.* **2006**, *35*, 637-659.
- ^{xvii} Pedersen, C. J. The Discovery of Crown Ethers (Nobel Lecture). *Angew. Chem., Int. Ed. Engl.* **1988**, *27*, 1021-1027.
- ^{xviii} Lehn, J.-M. Supramolecular Chemistry – Scope and Perspectives: Molecules, Supermolecules, and Molecular Devices (Nobel Lecture). *Angew. Chem. Int. Ed. Engl.* **1988**, *27*, 89-112.
- ^{xix} Cram, D. J. The Design of Molecular Hosts, Guests, and Their Complexes (Nobel Lecture). **1988**, *27*, 1009-1020.
- ^{xx} Diamond, D.; Nolan, K. Calixarenes: Designer Ligands for Chemical Sensors. *Anal. Chem.* **2001**, *73*, 22A-29A.
- ^{xxi} Clark, R. F.; Williams, S. R.; Nordt, S. P.; Manoguerra, A. S. A Review of Selected Seafood Poisonings. *Undersea Hyperb. Med.* **1999**, *26*, 175-184.
- ^{xxii} Fraley, A.; Ripp, S.; Sayler, G. S. Bioluminescent Bioreporter Sensing of Foodborne Toxins. *Genetically Engineered and Optical Probes for Biomedical Applications II*, Ed. Savitsky, A. P.; et. al. *Proc. of SPIE* **2004**, *5329*, 132-136.
- ^{xxiii} (a) Delangle, P.; Mulatier, J.-C.; Tinant, B.; Declercq, J.-P.; Dutasta, J.-P. Synthesis and Binding Properties of *iiii* (4i) Stereoisomers of Phosphonate Cavitands – Cooperative Effects in Cation Complexation in Organic Solvents. *Eur. J. Org. Chem.* **2001**, 3695-3704. (b) Dutasta, J.-P. New Phosphorylated Hosts for the Design of New Supramolecular Assemblies. *Top. Curr. Chem.* **2004**, *232*, 55-91.
- ^{xxiv} Topiol, S.; Weinstein, H.; Osman, R. A Theoretical Investigation of Histamine Tautomerization. *J. Med. Chem.* **1984**, *27*, 1531-1534.
- ^{xxv} Kong, J.; Dai, H. Full and Modulated Chemical Gating of Individual Carbon Nanotubes by Organic Amine Compounds. *J. Phys. Chem. B.* **2001**, *105*, 2890-2893.
- ^{xxvi} Tekarli, S.; Cundarii, T.; Omary, M. Rational Design of Macrometallocyclic Trinuclear Complexes with Superior π -Acidity and π -Basicity. *J. Am. Chem. Soc.* **2008**, *130*, 1669-1675.
- ^{xxvii} Sartori, P.; Golloch, A. Darstellung und Eigenschaften von Tetrafluorophthalsäure-Derivaten. *Chem. Ber.* **1968**, *101*, 2004-2009.
- ^{xxviii} Minghetti, G.; Banditelli, G.; Bonati, F. Metal Derivatives of Azoles, 3. The Pyrazolato Anion (and Homologues) as a Mono- or Bidentate Ligand: Preparation and Reactivity of Tri-, Bi-, and Mononuclear Gold(I) Derivatives. *Inorg. Chem.* **1979**, *18*, 658-663.

^{xxix} Schuster, D. I.; Megiatto, J. D. Nanotubes Reveal All in Solution. *Nature Chem.* **2009**, *1*, 243-249.

^{xxx} Rajesh, C.; Majumder, C.; Mizuseki, H.; Kawazoe, Y. A Theoretical Study on the Interaction of Aromatic Amino Acids with Graphene and Single Walled Carbon Nanotube. *J. Chem. Phys.* **2009**, *130*, 124911.

^{xxxi} Ganji, M. D.; Afsari, A. Interactions of Alkanethiols with Single-Walled Carbon Nanotubes: First Principles Calculations. *Physica E* **2009**, *41*, 1696-1700.

Curriculum Vitae of Kristin Lena Glab

Education

August 2007 – present: Massachusetts Institute of Technology, Cambridge, MA

August 2004 – May 2007: Vanderbilt University, Nashville, TN

- B.S. *summa cum laude*, high honors, chemistry major, mathematics minor

September 2000 – May 2004: University of Minnesota, Minneapolis, MN

- Non-degree seeking student

Scholarships and Awards

- 2007 National Science Foundation Graduate Research Fellowship award
- 2007 Joel Tellinghuisen Phi Beta Kappa Award for outstanding research accomplishments
- 2007 Outstanding Senior in Chemistry Award, Department of Chemistry, Vanderbilt University
- 2007 Donald E. Pearson Award for the most distinguished undergraduate research career in chemistry, Department of Chemistry, Vanderbilt University
- 2006 Barry M. Goldwater Scholar
- 2004 Dean's Select Scholarship, Vanderbilt University College of Arts and Sciences

Peer-Reviewed Publications

- Piecek, W.; Glab, K. L.; Januszko, A.; Perkowski, P.; Kaszynski, P. "Modification of electro-optical properties of an orthoconic chiral biphenyl smectogen with its isostructural carborane analogue." *Journal of Materials Chemistry* **2009**, *19*, 1173-1182.
- Januszko, A.; Glab, K. L.; Kaszynski, P. "Induction of smectic behavior in a carborane-containing mesogen. Tail fluorination of a three-ring nematogen and its miscibility with benzene analogues." *Liquid Crystals* **2008**, *35*, 549-553.
- Januszko, A.; Glab, K. L.; Kaszynski, P.; Patel, K.; Lewis, R. A. Mehl, G. "The effect of carborane, bicyclo[2.2.2]octane and benzene on mesogenic and dielectric properties of laterally fluorinated three-ring mesogens." *Journal of Materials Chemistry* **2006**, *31*, 3183-3192.

Selected Presentations

- Sly, J.; Bonifacio, C. S.; Chang, L.; Glab, K. L.; Lee, V. Y.; McNeil, M.; Jefferson, C. Michael; Frommer, Jane E.; Risk, William P.; Miller, Robert D. "Reaching for the stars: Layered polyvalent self-assembly of hyperbranched pigment arrays." *234th ACS National Meeting*, Boston, MA, August, **2007**; PMSE 121.
- Glab, K. L.; Kaszynski, P.; Piecek, W.; Januszko, A.; Patel, K.; Dziaduszek, J.; Drzewinski, W.; Mehl, G. H. "Fine-tuning of liquid crystals with carborane and fluorine substitution." *232nd ACS National Meeting*, San Francisco, CA, September, **2006**; ORGN 53.
- Glab, K. L.; Mueller, R.; Kauffman, K.; Meiler, J. "Novel Monte Carlo sampling and knowledge-based scoring approach for small molecule conformations." *232nd ACS National Meeting*, San Francisco, CA, September, **2006**; COMP 267.
- Glab, K. L.; Nguyen, S. T. "Synthesis of C27-C40 of the azaspiracids." *ACS 57th Southeast/61st Southwest Joint Regional Meeting*, Memphis, TN, October, **2005**; NOV04-454.